

Confinement effect on scattering states in a thin lead film: Field-induced resonance states in the high-bias regime of scanning tunneling microscopy

Hui Liu,¹ Jun Yan,^{1,2} Hongwu Zhao,¹ Shiwu Gao,^{1,2,*}† and Dongmin Chen^{1,*}‡

¹Beijing National Laboratory for Condensed Matter Physics and Institute of Physics, Chinese Academy of Sciences, Beijing 100080, China

²Department of Physics, Göteborg University, SE-412 96 Göteborg, Sweden

(Received 13 August 2007; published 7 September 2007)

Field-induced resonance states in the high-bias regime of scanning tunneling microscopy are used to couple and probe the scattering states above the vacuum level in a thin lead film. The resonance energies show a bilayer oscillation as a function of film thickness. Theoretical modeling unveils that the oscillation results from the confinement of the highly excited scattering states by the quantum well, yielding a bilayer phase modulation at the boundaries where they are coherently coupled to the external states.

DOI: [10.1103/PhysRevB.76.113403](https://doi.org/10.1103/PhysRevB.76.113403)

PACS number(s): 73.21.Fg, 73.40.Gk, 68.37.Ef

Highly excited scattering states in solid materials play important roles in various dynamical phenomena. These states typically occupy an energy continuum and are characterized by short lifetime (on the femtosecond scale), large momentum, and long-range extension in their wave functions. A wealth of knowledge has been gained on excitation and relaxation processes of low-energy excited states below the vacuum level.¹⁻³ It is relatively unexplored, however, how spatial confinement, such as in an ultrathin film or in an ultrathin layer in a heterostructure, interplays with these highly excited states. Quantum size effects^{4,5} are now well established phenomena in nanostructures. Can the spatial confinement lead to some unique properties of these highly excited scattering states in a quantum well (QW) structure, particularly when they are coherently coupled to the external states?

Indeed, a recent application of scanning tunneling microscopy in the field-emission mode has shown that resonant peaks in the tunneling spectra taken on a Ag layer exhibit “Stark shift” and secondary peaks that depend on the layer thickness.^{6,7} These are clear evidence that QW structures have influence on the states with energies well above the vacuum level. In this Brief Report, we extend a similar technique⁸⁻¹⁰ to probe the coherent coupling between internal scattering states of a thin Pb film and the field-induced states in the tunneling gap between the tip and the sample. As shown below, we observed a bilayer oscillation in the resonant energies as a function of film thickness, and thus provide solid evidence that these resonances are related to the internal scattering states in the film and not just a surface effect. Similar phenomena have been found, so far, only for the bound state electrons due to the quantum size effect.^{4,11} Based on a theoretical model, which exactly solves all scattering states in a unified one-dimensional potential, the measured tunneling resonances are shown to provide direct information of the scattering states. In particular, the modulation of tunneling resonances is found to be related to the phases of the scattering state at the boundaries where they couple to the external states. These phases are directly affected by the depth and width of the potential well, i.e., a confinement effect on the scattering states. While quantum confinement leads to discrete energy states for the bound

electrons, for the scattering states with a continuum energy spectrum, the confinement dictates which states can form resonant coupling with the external states.

Conventional scanning tunneling spectroscopy (STS) probes the bound states near the Fermi level. When the bias exceeds the vacuum level of the sample, field-induced states (FISs) formed between the tip and the sample, resulting in a set of resonant peaks in the tunneling spectroscopy.¹²⁻¹⁶ Here, we show that these FISs can couple to the continuum scattering states inside the film. By varying the tip-sample distance or bias, we can tune the energy levels in the tunneling gap. They in turn select out different scattering states inside the films with which the tip couples. We have chosen Pb films for our study because their quantum size effects for the bound states are well studied.^{4,11,17}

The experiments were carried out in an ultrahigh vacuum scanning tunneling microscopy (STM) system with a base pressure of 2.1×10^{-10} Torr. It is equipped with standard tools for *in situ* sample preparation, surface analysis, and a homemade STM operating from 5 K to room temperature (RT). The Si(111)-(7×7) surface was formed by degassing at 500–600 K for 12 h followed by a few cycles of heating to 1500 K. Pb was evaporated from a tantalum boat while keeping the Si(111) substrate at RT. The Pb film was checked by the Auger spectroscopy and was free of impurities. The dI/dV spectroscopy was performed using a lock-in technique with a 1.2 kHz 10 mV peak-to-peak modulation of the tip bias. All measurements were carried out at $T=77$ K. The layer thickness is determined by direct measurement with STM as well as by comparing the I - V curve with known data in the literature.^{11,17}

Figure 1(a) shows the STM topography image of a Pb wedge island grown on the Si(111)-(7×7) surface with thickness varying from 11 to 14 ML (monolayer) above the wetting layers. The step edges of the silicon terraces are indicated. Figure 1(b) shows the dI/dV map as a function of film thickness from 11 to 14 ML [across the solid line of Fig. 1(a)] and the tunneling gap voltage V_g from 0.1 to 4.0 V with a 10 mV step. Here, the white regions are the peaks in the density of states (DOS) above the Fermi level and up to five states are observed within 4 V of the gap voltage. Note that the peaks of DOS for the even number of Pb layers shift

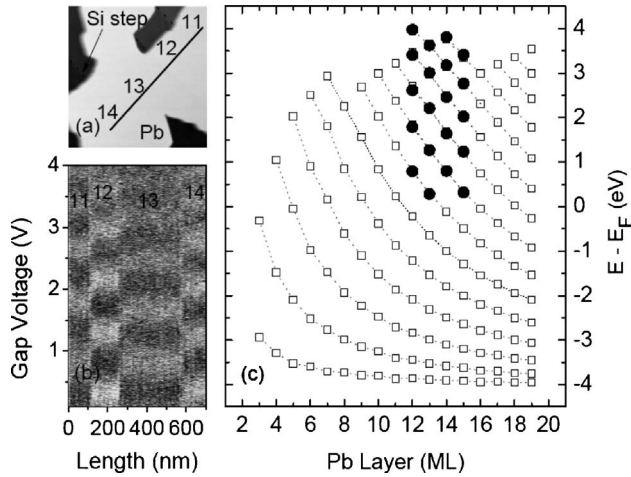


FIG. 1. $7000 \times 7000 \text{ \AA}^2$ STM image of a Pb wedge island on stepped Si(111) taken with $V_g = 2.0 \text{ V}$ and set current $I = 0.8 \text{ nA}$. (b) dI/dV map as a function of V_g and Pb thickness from 11 to 14 ML scanned along the line marked in (a) with loop closed and set current $I = 0.8 \text{ nA}$. (c) Layer dependent quantum well states' energies obtained by *ab initio* calculation (in open square) in comparison with the experimental data (solid circle) extracted from (b).

a half way between two adjacent peaks of the odd number layers and the dI/dV map in Fig. 1(b) clearly exhibits a bilayer periodicity. From previous work,¹⁷ it is well understood that the observed electronic states are the unoccupied QW states confined between the sample surface and the Pb/Si(111) interface. Figure 1(c) shows that the energies of these states obtained from the dI/dV spectra fit well with the theoretical values from our *ab initio* calculation using Vienna *ab initio* simulation package (VASP).^{18,19} Note that the unoccupied QW states can be mapped out by tunnel electrons all the way up to the vacuum level.

When V_g exceeds the work function of the sample, electrons tunneling out of the tip will propagate in the tunneling gap and form standing waves as reported previously.¹³⁻¹⁶ Figure 2(a) plots the typical dI/dV and z spectra as a function of V_g from 3.0 to 8.0 V. Unlike the conventional STS, the feedback loop of the STM was kept closed while ramping the bias in order to accommodate a large dynamic range of V_g . To maintain a constant tunneling current, the tip height Z (solid curve) is raised by the servo with increasing gap voltage. When V_g (and Z) matches the energy of an FIS, there is an increase in the tunneling current and hence a sharp rise in the tip-sample distance, as manifested in Fig. 2(a). Over the center of a 13 ML island, we observed up to six FISs at a tunneling current of 0.8 nA. The $n=1$ level of the FIS is identified by the first step in the Z - V spectroscopy.

Figure 2(b) plots the Pb thickness dependent dI/dV spectroscopy taken along the same line as marked in Fig. 1(a) with $I = 0.8 \text{ nA}$ (right hand panel) and V_g varying from 5.0 to 8.0 V with a 10 mV step. We found a total of six FISs, similar to those reported in Ref. 7, counting their secondary peaks as well. The main difference is due to a lower electric field in the tunnel gap for our cases, which yields more FISs in the similar energy range. Quite remarkably, we found that the FIS ($n=1-6$) peak positions oscillate as a function of

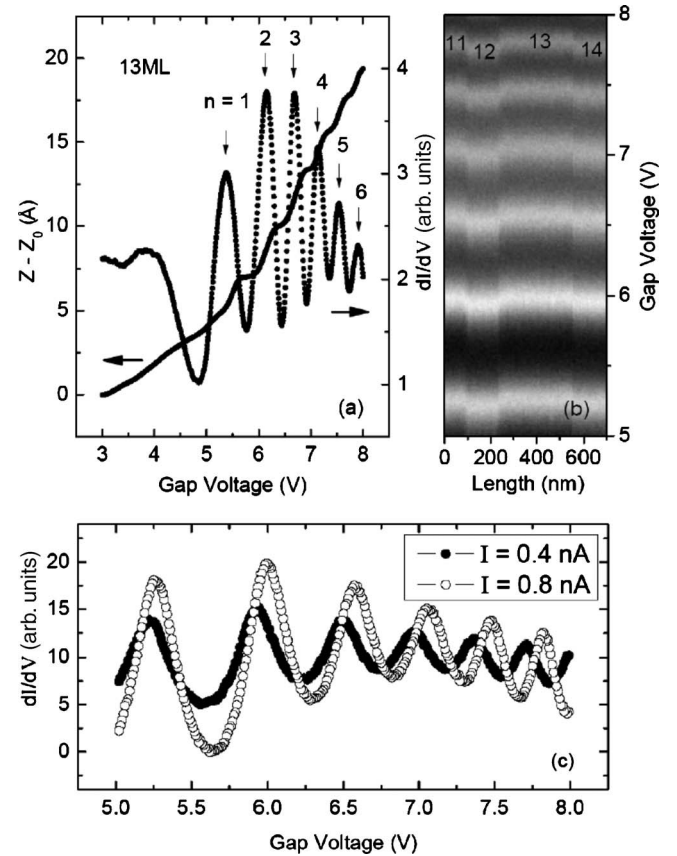


FIG. 2. (a) The measured closed-loop Z - V and dI/dV spectra on 13 ML Pb with a set current of 0.8 nA. Z_0 is the tip-sample distance at $V_g = 3.0 \text{ V}$. (b) dI/dV map as a function of Pb layers (11–14 ML) scanned along the same position as in Fig. 1(b) but at a higher V_g (5.0–8.0 V) with a set current of 0.4 nA. (c) The resonant tunneling spectra acquired on 13 ML Pb with the tunneling current set at 0.4 and 0.8 nA.

thickness. The odd layers (11 and 13 ML) yield FISs with energies about 30 meV higher than those of even layers (12 and 14 ML). Similar thickness dependence of dI/dV spectroscopy was obtained with a lower set current of 0.4 nA on the same sample. At the same Pb thickness, the FIS shifted to lower energies, as shown in Fig. 2(c), due to the reduction of the electric field in the gap, also known as the Stark shift observed.^{6,7}

The bilayer modulation of the FIS energy spectra has not been reported for bulk samples¹³⁻¹⁶ or for the thin Ag film on the Si(111)-(7 \times 7).^{6,7} It is clear that energy spectra of the FISs on thin films are closely associated with the number of ML of these films. A model that treats the thin film and the tunnel gap separately will not be able to accurately account for the full quantum mechanical nature of the system. We thus consider a model where the FISs in the tunneling gap and the continuum scattering states inside the film are treated on equal footing in a unified one-dimensional (1D) potential model, as illustrated in Fig. 3 (solid line). The Pb film was described by a 1D square well with variable width, augmented with a linear (triangle) potential in the tunneling gap. The depth of the QW was approximated by the sum of the p -band width (3.9 eV) and the work function (3.8 eV),

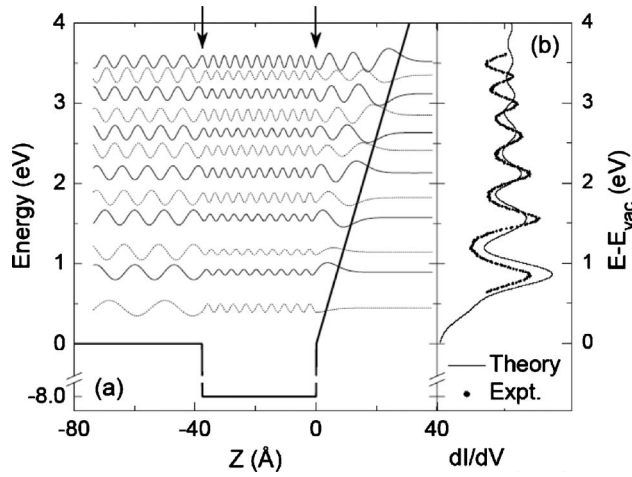


FIG. 3. (a) The model potential (heavy solid line) and representative wave functions as a function of eigenenergy (the vertical axis). The thin Pb film is modeled by a square well with a depth of 8 eV and a variable thickness D [$D=n(2.9 \text{ \AA})$, n being the number of layers]. The two arrows mark the Pb film boundaries. The linear potential to the right describes the electric field in the tunneling gap. The field strength is modeled by a slope of 0.13 eV/\AA for a 0.4 nA set current. (b) The calculated local density of states (LDOS) as measured by the tip is compared with the measured dI/dV curve at 0.4 nA . The LDOS was obtained by projecting the wave functions of all states to the tip, and a Lorentzian broadening with 0.4 eV is used in the summation over states.

which were obtained from the *ab initio* band structures for the Pb(111) film.^{18,19} The slope of the linear potential, the electric field, was determined from the Z - V measurement. Only freestanding Pb films were considered in this model, which yields vacuum on the substrate side since the shift in FIS energies was contributed mainly by coupling between the FISs in the tunneling gap and the scattering states inside the film, and less from the substrate. The continuum spectra of the scattering states were discretized in the momentum space so that the energy spectrum is quasicontinuum with a level spacing smaller than 0.15 eV . Such a continuum spectrum is essential to provide sufficient number of scattering states that couple with the FIS in the tunneling gap.

Figure 3 shows the wave functions at a few selected energies for a 13 layer Pb slab [Fig. 3(a)] and the projected local density of states (LDOS) compared with that probed by the STM [Fig. 3(b)]. Due to the potential profile, these wave functions show three typical features: (i) free scattering states outside the lead film (left), (ii) standing waves inside the QW, and (iii) Airy-like wave functions in the tunneling gap. These states are continuous in energy spectrum, as they are well above the vacuum level. Their LDOSs as probed by the STM [Fig. 3(b)] are, however, characterized by a set of peaks and valleys corresponding to the states in resonance (solid line) and out of resonance (dotted line) in Fig. 3(a). We shall unveil below that the dI/dV spectra not only relate to the FIS⁶⁻¹⁰ due to the confinement by the linear potential in the tunneling gap but also couple strongly to the Pb QW structure. With a slope of 0.13 eV/\AA determined by our experiment, the LDOS spectrum well reproduces the resonance

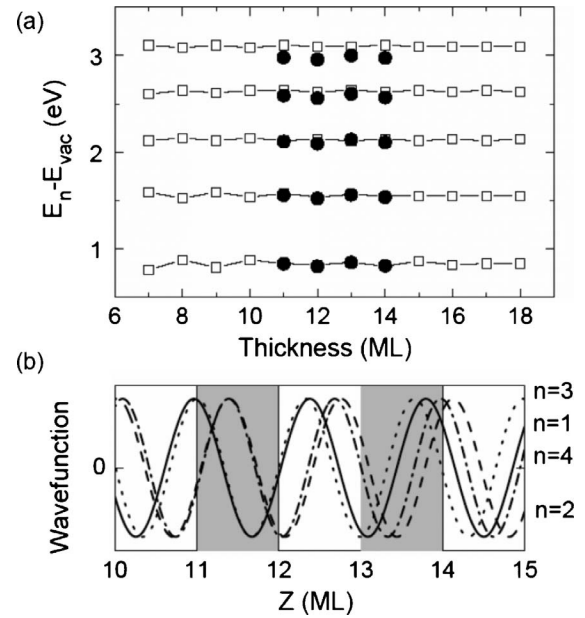


FIG. 4. (a) Calculated (hollow square) and measured (solid circle) resonant energies, for the lowest four states above the vacuum level, are shown as a function of thickness. (b) The wave functions plotted with energy fixed at that of $n=1$ FIS of 11 ML (solid lines) and at their corresponding $n=1$ FIS resonant energy for each thickness (dashed lines).

peaks measured by the dI/dV spectroscopy for a 13 ML Pb film as shown in Fig. 3(b). For higher resonant states ($n \geq 5$), the calculated energies are slightly higher than the experimental values, which may be attributed to possible nonlinear dependence between the electric field and bias as the tip retracted from the sample at increased bias. Indeed, the resonance energies at higher bias can be better fitted with a lower field strength of 0.10 eV/\AA . In our calculation, such nonlinearity of the electrostatic potential was neglected in order to keep the model as simple and instructive as possible.

Figure 4(a) shows the calculated FIS energies for the lowest four states as a function of thickness for up to 18 layers, which show excellent agreement with the experiment for 11–14 ML. In particular, the bilayer modulation in resonance energies is in agreement with the experimental data in both sign and amplitude. The amplitude of modulation is stronger in thinner films (7–10 ML), $\sim 30 \text{ meV}$, and decays gradually as the thickness increases. This bilayer modulation has an origin different from that of the oscillations observed for the ground states.^{4,11} Figure 4(b) plots the wave functions of the $n=1$ FIS from 11 to 14 ML. The solid lines are the wave functions with energy fixed at that of 11 ML. They are the “unmodulated” $n=1$ FISs at these thicknesses. For comparison, the dashed lines are the wave functions for the “modulated” $n=1$ state, whose energies were chosen at the $n=1$ resonance peak of the corresponding thickness. By a minor modulation in energy, the phase of the wave function adjusts at the two boundaries, especially at $n=12$ and 14 ML. It results in a significant enhancement in the amplitude inside the film and in the gap region. This modulation trend has been observed for all the lowest four states we calculated.

This phase matching picture can be further supported by analyzing the FIS wavelengths, which are 4.10, 3.96, 3.84, and 3.75 Å for $n=1-4$. Increasing the thickness by 1 ML adds a phase of about $3\pi/2$ to the electron standing waves inside the film. It thus gives a bilayer oscillation. This oscillation period is different from that in the bound state, where the phase changes approximately by $\pi/2$ when the thickness changes by one layer.^{4,11} It is due to the fact that the electron momenta for the highly excited states are about three times shorter than those of the states near the Fermi level.

We thus conclude that the observed bilayer modulation in the dI/dV spectra at high bias results from a coherent coupling, or phase matching, between the field-induced image states and the scattering states in the Pb QW structure. This coupling, though weakly modulated in energies (for up to 30 meV), is rather long ranged and does not die out for up to 20 ML, as observed in the low-lying resonances.⁴ Such a long-range coupling between the FISs and the highly excited states in the QW provides a unique way to probe the electronic excitations within a QW using resonance tunneling

spectroscopy. Finally, by adjusting the set current in the tunneling spectroscopy, it is possible to select out and probe a range of internal excitation energies in a QW as shown in Fig. 2(c), making this technique quite useful indeed.

In conclusion, we show that spatial confinement of a QW structure can have important effects on the highly excited scattering states, just as it does on the bound states. Even though the energy spectra of the scattering states are continuous, the phases of their wave functions at the boundaries are quite sensitive to the depth and width of the QW at an atomic scale. This effect allows the internal excitations be coherently coupled to the external, such as the tunnel junction in an STM, and may be exploited in other types of applications.

This work was supported in part by the National Science Foundation of China (Grant No. 90406017), the 100-Talent program of Chinese Academy of Sciences, and the Institutional Grant Program by the Swedish Foundation for International Collaboration in Research and Higher Education.

*Authors to whom correspondence should be addressed.

†swgao@aphy.iphy.ac.cn

‡dmchen@aphy.iphy.ac.cn

¹U. Höfer, I. L. Shumay, Ch. Reuß, U. Thomann, W. Wallauer, and Th. Fauster, *Science* **277**, 1480 (1997).

²N.-H. Ge, C. M. Wong, R. L. Linger, Jr., J. D. McNeill, K. J. Gaffney, and C. B. Harris, *Science* **279**, 202 (1998).

³P. M. Echenique, R. Berndt, E. V. Chulkov, Th. Fauster, A. Goldmann, and U. Höfer, *Surf. Sci. Rep.* **52**, 219 (2004), and references therein.

⁴Y. Guo, Y.-F. Zhang, X.-Y. Bao, T.-Z. Han, Z. Tang, L.-X. Zhang, W.-G. Zhu, E. G. Wang, Q. Niu, Z. Q. Qiu, J.-F. Jia, Z.-X. Zhao, and Q.-K. Xue, *Science* **306**, 1915 (2004).

⁵T.-C. Chiang, *Surf. Sci. Rep.* **39**, 181 (2000).

⁶W. B. Su, S. M. Lu, C. L. Jiang, H. T. Shih, C. S. Chang, and T. Tsong, *Phys. Rev. B* **74**, 155330 (2006).

⁷W. B. Su, S. M. Lu, H. T. Shih, C. L. Jiang, C. S. Chang, and T. Tsong, *J. Phys.: Condens. Matter* **18**, 6299 (2006).

⁸K. Bobrov, A. J. Mayne, and G. Dujardin, *Nature (London)* **413**, 616 (2001).

⁹D. B. Dougherty, P. Maksymovych, J. Lee, and J. T. Yates, Jr., *Phys. Rev. Lett.* **97**, 236806 (2006).

¹⁰Th. Fauster and W. Steinmann, in *Photonic Probes of Surfaces*,

edited by P. Halevi (Elsevier, Amsterdam, 1995), pp. 347–411.

¹¹C. M. Wei and M. Y. Chou, *Phys. Rev. B* **66**, 233408 (2002).

¹²K. H. Gundlach, *Solid-State Electron.* **9**, 949 (1966).

¹³G. Binnig, K. H. Frank, H. Fuchs, N. Garcia, B. Reihl, H. Rohrer, F. Salvan, and A. R. Williams, *Phys. Rev. Lett.* **55**, 991 (1985).

¹⁴R. S. Becker, J. A. Golovchenko, and B. S. Swartzentruber, *Phys. Rev. Lett.* **55**, 987 (1985).

¹⁵S. Yang, R. A. Bartynski, G. P. Kochanski, S. Papadia, T. Fondén, and M. Persson, *Phys. Rev. Lett.* **70**, 849 (1993).

¹⁶P. Wahl, M. A. Schneider, L. Diekhöner, R. Vogelgesang, and K. Kern, *Phys. Rev. Lett.* **91**, 106802 (2003).

¹⁷I. B. Altfeder, K. A. Matveev, and D. M. Chen, *Phys. Rev. Lett.* **78**, 2815 (1997).

¹⁸G. Kresse and J. Hafner, *Phys. Rev. B* **47**, 558 (1993); **49**, 14251 (1994); *J. Phys.: Condens. Matter* **6**, 8245 (1994).

¹⁹The theoretical lattice constant for Pb is 5.03 Å. Half ML was added on each side of the slabs which yields one ML's shift in Fig. 1(c). The same vacuum region equal to five Pb layers was used. All the atoms were geometrically fully relaxed. The Brillouin zone was sampled using a $13 \times 13 \times 1$ k -point grid and the plane-wave basis set was truncated at a kinetic energy of 100 eV.